Available online at www.sciencedirect.com
ScienceDirect
Applied Surface Science 252 (2006) 8598–8604
applied surface science
www.elsevier.com/locate/apsusc

The removal of sodium dodecylbenzene sulfonate surfactant from water using silica/titania nanorods/nanotubes composite membrane with photocatalytic capability

Haimin Zhang, Xie Quan *, Shuo Chen, Huimin Zhao, Yazhi Zhao

School of Environmental and Biological Science and Technology, Dalian University of Technology, Linggong Road 2, Dalian 116024, PR China

Received 22 August 2005; received in revised form 28 November 2005; accepted 28 November 2005
Available online 19 January 2006

Abstract

This paper reports experimental results on removal of sodium dodecylbenzene sulfonate (SDBS), using silica/titania nanorods/nanotubes composite membrane with photocatalytic capability. This multifunctional composite membrane has been successfully prepared from colloidal *X*-silica/titania sols (*X* denotes molar percent of silica) by the sol–gel technique. The prepared nanorods/nanotubes composite membranes were characterized by X-ray diffraction (XRD), scanning electron microscope (SEM), scanning probe microscope (SPM) and UV–vis diffuse reflectance spectra (DRS). XRD patterns confirmed that the embedding of amorphous silica into nanophase titania matrix helped to increase the thermal stability of titania and control the size of titania particles. The small size titania particles with anatase phase played an important role in formation of silica/titania nanorods/nanotubes composite membranes with photocatalytic capability. The percentage of anatase phase titania reached 93% when 20%-silica/titania nanorods/nanotubes composite membrane calcined at 400 °C for 2 h. Most (95%) of the pore volume was located in mesopores of diameters ranging from 1.4 to 10 nm. The experimental results showed that the removal of SDBS achieved 89% after 100 min by combining the photocatalysis with membrane filtration techniques. Although the SDBS was not completely decomposed by photocatalysis, the degradation of the SDBS helped to enhance composite membrane flux and prevent membrane fouling. It was possible to treat successfully surfactant wastewater using multifunctional silica/titania nanorods/nanotubes composite membrane by means of a continuous process; this could be interesting for industrial applications.

Keywords: Silica/titania composite membrane; Photocatalysis; Membrane separation; SDBS

1. Introduction

The presence of corrosive substances, solvents, organic compounds, metals, etc., in superficial waters is a serious problem worldwide [1,2]. Many methods of water treatment (removal of polluting agents) are in many cases expensive and inefficient. Therefore, exploring new methods and technologies of water treatment has attracted significant attention.

In recent years, the technology of membrane separation has already shown to be competitive with other separation processes for what concerns energy costs, material recovery, reduction of the environmental impact and achievement of integrated processes with selective removal of some components [3,4]. Membrane separation processes are suitable for application in many fields, such as the textile industry (to remove colouring agents) [5,6], food and pharmaceutical industry (for separation of mineral salts and small organic molecules) and wastewater recycling [7]. However, this method only transfers pollutants from a phase to another and only displays a simple separation function.

Over the past several years, TiO_2 nanostructures have become a focus of considerable interest because they possess unique properties relevant to applications including chemical sensing [8], photocatalysis [9] and photovoltaics [10]. TiO_2 photocatalysis proves to be a promising technology for the purification and treatment of both contaminated air and water [11]. Chen et al. have reported a novel TiO_2-based p–n junction nanotube photocatalyst, which shows excellent photoactivity [12]. Some multicomponent or mixed oxides such as $SrTiO_3$, $BaTiO_3$, TiO_2/ZrO_2, $K_2La_2TiO_3$, $Ni_2O_3/TiO_{2-x}B_x$, ZnO–ZnS

* Corresponding author. Tel.: +86 411 84706265; fax: +86 411 84706263.
E-mail address: zhmin1202@126.com (X. Quan).

0169-4332/$ – see front matter © 2005 Elsevier B.V. All rights reserved.
doi:10.1016/j.apsusc.2005.11.090

and silica–titania have good photoactivity [13–19]. Especially, silica–titania mixed oxide was used as not only a good photocatalyst itself but also a support material for other chemical reaction catalyst [20]. Although silica–titania mixed oxides have attracted considerable attention owing to their excellent photocatalytic activity for removal of organic contaminants, the separation of silica–titania particles creates another problem to be solved in practical applications of the process. A major difficulty in the separation of silica–titania particles from treated water arises because silica–titania particles are too fine to be removed by gravity settling. Attaching the catalysts to a suitable substrate can overcome the separation problem; however, the effective surface area of the catalysts will be decreased. Up-to-date studies on photocatalytic methods reported in literatures concern only the scientific aspects of this process and principally refer to batch systems where the catalyst is simply suspended in water. In the case of these systems there is need to recover the suspended solids. Therefore, the problem of separating photocatalysts cannot be neglected.

The major idea of this work is to explore the feasibility of combining the photocatalysis with membrane techniques for heterogeneous photocatalysis applications and understand this behaviour and to improve the performance of the membrane with photocatalytic function in order to take advantage of the benefits of both the photocatalysis and membrane technology for pollutants removal. Therefore, we prepared successfully silica/titania nanorods/nanotubes composite membranes with photocatalytic capability on the support of alumina by sol–gel technique. We found that the embedding of some portion of silica into titania particles increased the thermal stability of titania and inhibited the growth of titania particles size and the phase transformation of titania from anatase to rutile. The high thermal stability makes it possible to employ the silica/titania composite membrane at higher temperature while keeping the major phase as anatase. The small size titania particles with anatase phase may play an important role in formation of silica/titania nanorods/nanotubes composite membrane with photocatalytic capability. The silica/titania nanorods/nanotubes composite membranes on the support of alumina may have the multifunctions of separation and photocatalysis simultaneously. For this research, sodium dodecylbenzene sulfonate (SDBS) has been selected as the test pollutant, due to its widespread use in the manufacturing of products such as toothpaste, bath soaps, shampoos, etc.

2. Experiment

Tetra-*n*-butyl titanate [$Ti(OC_4H_9)_4$] and tetraethyl orthosilicate [98% $Si(OC_2H_5)_4$, TEOS, liquid] were AR grade and obtained from Shanghai Reagent Company. Ethanol (C_2H_5OH), NaOH, HCl and other chemicals were AR grade and obtained from Tianjin Kermel Chemical Reagents Development Centre. The water used was double distilled and then purified with the Milli-Q system. The substrate of sodium dodecylbenzene sulfonate was obtained from Tianjin Kermel Chemical Reagents Development Centre and used without further purification. The alumina template membranes with 200 nm diameter pores were obtained commercially (Whatman Anopore filters, Fisher, Anodisc 47).

Silica/titania nanorods/nanotubes composite membranes were prepared using a sol–gel method. 23.5 mL of $Ti(OC_4H_9)_4$ and *V* mL (*V* = 0, 2.25 and 4.5 mL) of $Si(OC_2H_5)_4$ were added to 23 mL of ethanol, and the resulting solution was stirred for 30 min at room temperature. A mixed solution of 23 mL of ethanol and 18 g of 4.4 mol/L HCl aqueous solution was added slowly to the mixed solution of $Ti(OC_4H_9)_4$, $Si(OC_2H_5)_4$ and ethanol.

The resulting mixture was kept standing at room temperature for hydrolysis reaction for 60 min, and then was irradiated with an ultrasonic cleaning bath for 10 min, resulting in a transparent and straw color silica/titania sol. The alumina template membrane was immediately dipped into this solution for a certain immersion time. After the desired immersion time, the membrane was removed from the sol and dried in air for 1 h at room temperature. The composite membranes and correspondingly dried *X*-silica/titania sol were then placed in a muffle furnace. The temperature was ramped to 400 °C (100 °C/h) and kept for 2 h, and then ramped back down (50 °C/h) to the room temperature.

All permeability and rejection measurements were evaluated using the membrane test unit, as shown in Fig. 1. The SDBS solution was pumped from a solution reservoir through the membrane cell and back to the reservoir. Permeate and retentate

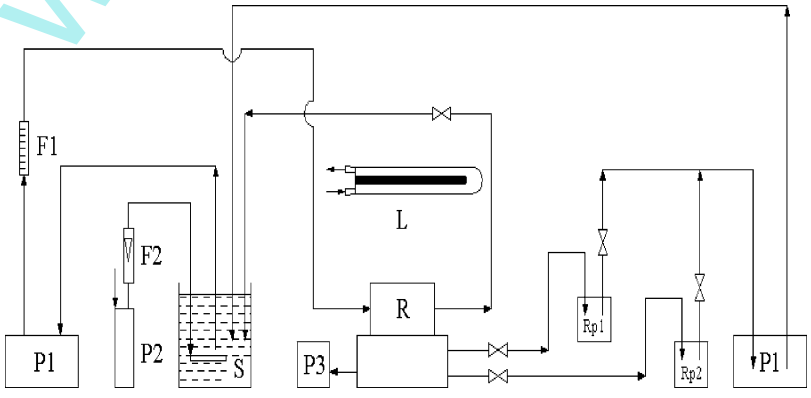

Fig. 1. Scheme of the experimental set-up (F1 and F2: flowmeters; P1: peristaltic pump; P2: air pump; P3: vacuum pump; S: re-circulation tank; Rp1 and Rp2: permeate reservoirs; R: membrane test cell; L: UV lamp).

were recycled. The temperature of the system was kept at 298 K. The flow velocity through test cell was kept at 12.7 L/h.

The experiment of photocatalytic reaction was conducted in the same membrane test unit (Fig. 1). When the photocatalytic reaction was performed, a 300 W high-pressure mercury lamp with a characteristic wavelength of 365 nm was used as UV source, which was surrounded by quartz cooling thimble (25 mm in diameter). The lamp was placed upper the reactor and the distance between its bulb and the surface of silica/titania nanorods/nanotubes composite membrane was 10 cm. The light intensity at this distance was 400 μW/cm^2. A 3 mL of sample was withdrawn at given reaction intervals, and was analyzed with a spectrophotometer at λ_{max} = 224 nm (UV absorption of the aromatic group) [21,22] and was returned quickly. During the experiment, air was bubbled into the solution using an inorganic ceramic microfiltration membrane (inner diameter = 8 mm, length = 50 mm and average pore diameter = 0.2 μm). The inorganic ceramic microfiltration membrane was able to maximize the exchange surface to achieve optimal air dissolution by means of microbubble formation. SDBS solution was stirred by air bubbling in darkness for 30 min to establish adsorption–desorption equilibrium before the experiments started.

The morphology of silica/titania nanorods/nanotubes composite membranes was observed using scanning electron microscope (SEM, JSM-5600LV, Oxford, UK). The surface morphology of silica/titania nanorods/nanotubes composite membranes was also observed on scanning probe microscope (SPM, CSPM-3000, China). The phases and structures of samples were identified by X-ray diffractometer (XRD, LabX-6000, Shimadzu, Japan) employing Cu Kα radiation at 40 kV and 30 mA over the 2θ range of 20–100°. UV–vis diffuse reflectance spectra (DRS) and concentrations of SDBS were obtained by UV–vis spectrophotometer (JASCO V-550, Japan). The pH value was controlled by acidimeter (Basic pH Meter PB-20, Sartorius, Germany).

3. Results and discussion

3.1. Characterization of X-silica/titania nanorods/nanotubes composite membrane

Fig. 2 shows XRD patterns of the prepared *X*-silica/titania composite membranes with different silica contents at 400 °C for 2 h. For pure titania, significant peaks of rutile phase are observed obviously at 400 °C. Brookite phase of titania is also observed obviously for pure titania and the peak intensity of brookite phase decreases with increasing silica content. The dominant phase of titania is anatase when some portion of silica is embedded into titania particles. No significant peaks of rutile and no peaks of silica crystal are observed for all silica/titania ratios (except pure titania) as shown in Fig. 2. It is confirmed that the silica/titania composite has high thermal stability, which results in the suppression of phase transformation of titania from anatase to rutile. The size of the crystallites can be determined from the broadening of corresponding X-ray diffraction peaks by using Scherrer

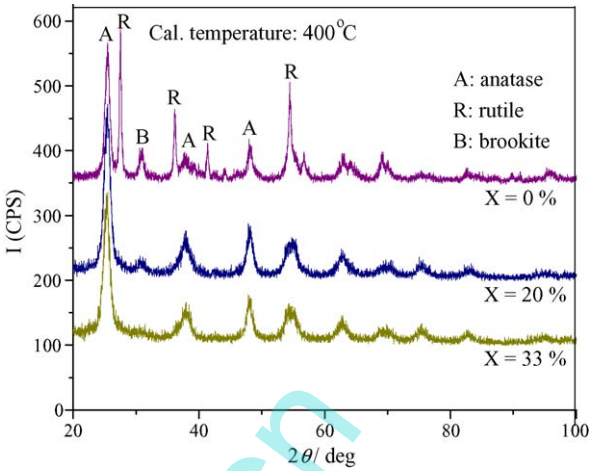

Fig. 2. XRD patterns of *X*-silica/titania composite membranes with changing the silica content (*X*) at 400 °C.

formula $D = (K\lambda)/(\beta \cos\theta)$, where λ is the wavelength of the X-ray radiation (λ = 0.15406 nm), *K* the Scherrer constant (*K* = 0.89), θ X-ray diffraction peak and β is the full-width at half-maximum (FWHM) of the (1 0 1) plane (in radians). The sizes of titania particles are 23, 6.9 and 6.8 nm for silica contents of 0, 20 and 33%, respectively. There is no significant change in the size of silica/titania particles with changing the silica contents (except pure titania). This result confirms that the embedding of some portion of silica into titania particles inhibits the growth of anatase crystal of titania particles. The small size titania particles with anatase phase are very beneficial for the formation of silica/titania nanorods/nanotubes composite membrane with photocalytic capability.

Fig. 3a shows scanning electron micrographs of the surface of the 20%-silica/titania nanorods/nanotubes composite membrane with immersion time of 10 min. As shown, there are many fine and uniform pores in the membrane. Fig. 3b is a SEM image of the cross-section of the 20%-silica/titania composite membrane, and the thickness is approximately 60 μm. However, the silica/titania layers cannot be observed obviously from the image of the cross-section. This may be because the silica/titania layers are very thin. In order to investigate silica/titania nanotubes microstructures in the inside of 20%-silica/titania composite membrane, one surface layer of the composite membrane was removed, and the membrane was glued to a piece of filter paper with the polished face up. The resulting composite was immersed into 6 mol/L NaOH solution for 5 min at 50 °C to dissolve the alumina, and then rinsed with 1 mol/L HCl and deionized water sequently. Fig. 3c shows SEM image of silica/titania nanotubes (×10,000 and ×50,000) in the alumina membrane. It can be seen from Fig. 3c that the nanotubes are about 60 μm long with outer diameters of 200 nm. Most of the nanotubes observed in SEM investigation are shorter than 60 μm and unordered, which may be attributed to the break of the nanotubes during the preparation of the SEM samples. The morphology of the surface of the 20%-silica/titania nanorods/nanotubes composite membrane was further observed by SPM (Fig. 3d). SPM micrograph shows silica/titania particles with rod-shaped homogenously distributed on

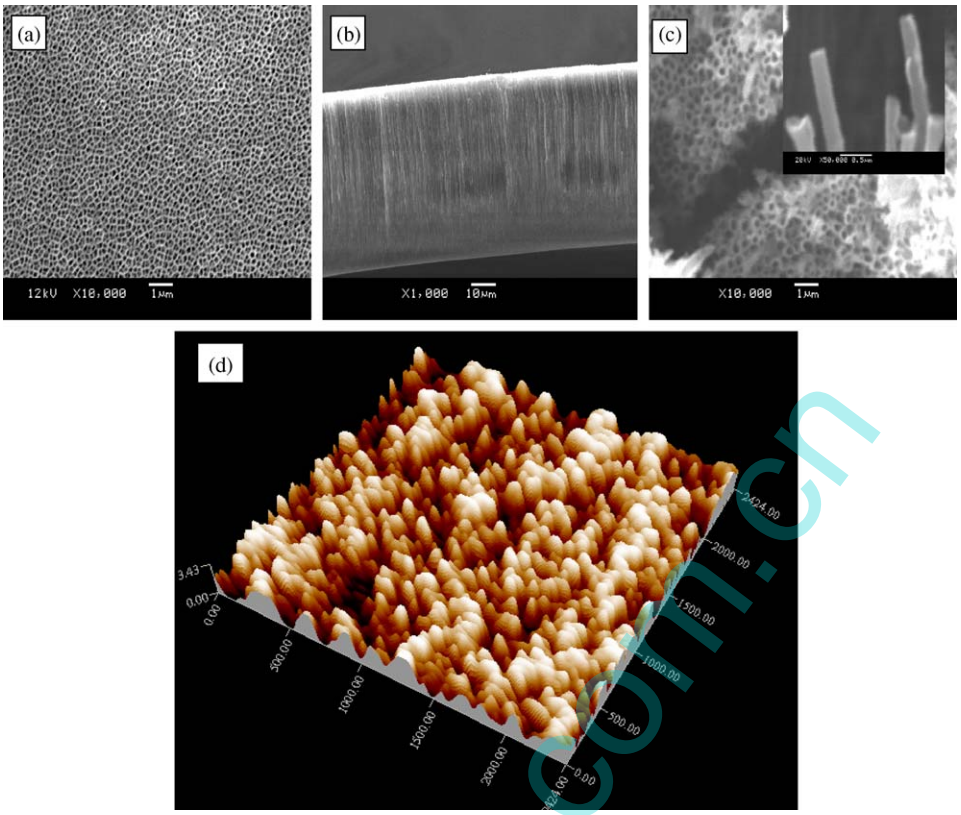

Fig. 3. Electron photographs of the surface and the cross-section of 20%-silica/titania composite membrane and 20%-silica/titania nanotubes prepared in the alumina membranes with 200 nm diameter pores. The sol was maintained at 20 °C, and the immersion time was 10 min. SEM photograph of: (a) the surface of 20%-silica/titania composite membrane; (b) the cross-section of 20%-silica/titania composite membrane; (c) 20%-silica/titania nanotubes (×10,000 and ×50,000); (d) SPM photograph of the surface of 20%-silica/titania composite membrane.

the support of alumina and the silica/titania nanorod is about 5 nm high (the thickness of silica/titania layer). It can be also seen from Fig. 3d that there are some larger pores in the silica/titania composite membrane. According to pore size distribution analysis of the 20%-silica/titania nanorods/nanotubes composite membrane, the pore size distribution of composite membrane is correspondingly wide ranging from 1.0 to 30 nm. But most (95%) of the pore volume is located in mesopores of diameters ranging from 1.4 to 10 nm. It is these mesopore structures that allow rapid diffusion of various products during UV illumination and enhance the rate of photocatalytic reaction.

In order to determine the composition of nanotubes, energy dispersive X-ray spectra (EDX) experiments were performed on 20%-silica/titania nanotubes. Fig. 4 shows the typical EDX spectra from the sample. Only Ti, Si and O peaks are observed in the spectra. Strong Kα and Kβ signals from Ti are seen at 4.51 and 4.93 keV, respectively. The Kα peak from O and Kα peak from Si are also observed at 0.52 and 1.74 keV, respectively. Ignoring the possible existence of undetectable light elements such as H in the sample, the nanotubes may be concluded to be composed of mainly Ti, Si and O. Previous study on FT-IR spectra of 20%-silica/titania composite proved that silica phase did not exist as segregated phase, but formed Ti–O–Si group in the matrix of anatase-phase titania. Similar result was obtained by Jung and Park [23].

The UV–vis absorption spectrums of 20%-silica/titania nanorods/nanotubes composite membrane, 20%-silica/titania powder, 33%-silica/titania powder, pure titania and uncoated alumina membrane indicate the maximum absorption wavelengths are around 260, 320, 320, 340 and 340 nm, respectively (shown in Fig. 5). The band gap absorption edges of 20%-silica/titania nanorods/nanotubes composite membrane, 20%-silica/

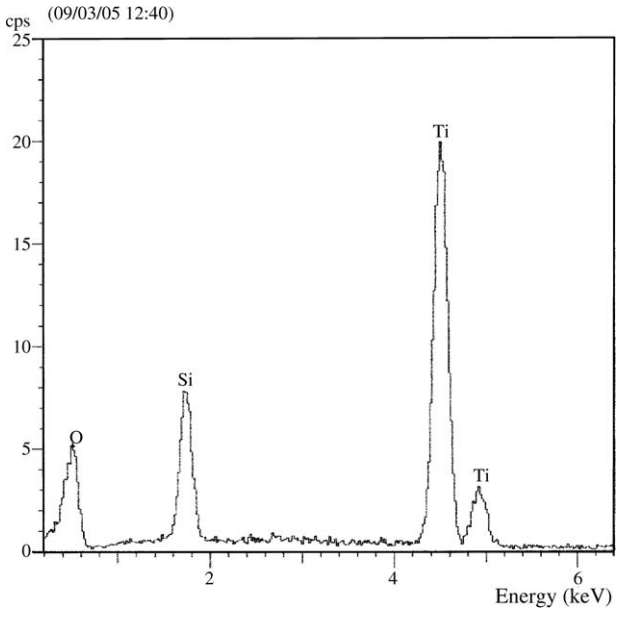

Fig. 4. Selected area energy dispersive X-ray spectra of individual nanotube.

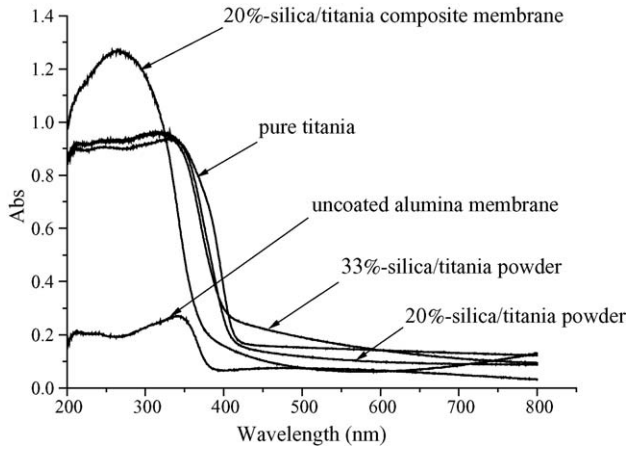

Fig. 5. Diffuse reflectance UV–vis spectra of the samples calcined at 400 °C for 2 h.

titania powder, 33%-silica/titania powder, pure titania and uncoated alumina membrane are around 370, 410, 410, 420 and 370 nm, respectively, and the band gap energies calculated with Kubelka–Munk function [24] is about 3.3, 3.0, 3.0, 2.95 and 3.3 eV, respectively. The above results imply that the support of alumina membrane may play an important role for the significant blue-shift with higher band energy of the 20%-silica/titania nanorods/nanotubes composite membrane. Moreover, the absorption intensity of the 20%-silica/titania nanorods/nanotubes composite membrane is obviously higher than that of silica/titania powder, pure titania and uncoated alumina membrane, which may be very beneficial for the photocatalytic degradation of organic pollutants under UV irradiation.

3.2. Permeability and rejection experiments of 20%-silica/titania nanorods/nanotubes composite membrane

Membrane rejection was investigated using high molar mass PEG. This characterization method was chosen because many publications have shown that this is a very reliable and easily reproducible method [25]. Various PEG fractions with an average molar mass of 6000, 10,000 and 20,000 g/mol were used. The concentration of all fractions in the reservoir is 500 mg/L. The experiments were performed at 298 K and at a pressure difference of 0.05 MPa.

The concentration of PEG fractions in the feed and the permeate solution was determined by the values of chemical oxygen demand (COD). Retention for each molar mass was calculated by the following equation:

$$R_i = \left[1 - \left(\frac{C_{i,\text{permeate}}}{C_i}\right)\right] \times 100$$

Fig. 6 shows different PEG fractions retention of 20%-silica/titania nanorods/nanotubes composite membrane. The retention of the PEG fractions increases as molar mass of the PEG fractions increases. For 20%-silica/titania nanorods/nanotubes composite membrane, measurements using PEG show 36, 65 and 89% retentions of 6000, 10,000 and 20,000 g/mol at a pressure difference of 0.05 MPa, respectively. For all PEG fractions, the 20%-silica/titania nanorods/nanotubes composite membrane shows a steady retention after 60 min.

Fig. 7 shows SDBS solutions permeation flux and retention at pH 3.5 of 20%-silica/titania nanorods/nanotubes composite membrane at a pressure difference of 0.05 MPa. As shown, the permeation flux of the 20%-silica/titania nanorods/nanotubes composite membrane decreases as time increases. Nevertheless, after 60 min filtration, the permeation flux of the 20%-silica/titania nanorods/nanotubes composite membrane is almost steady (47 L/(m^2 h)). The steady retention reaches 74% after 100 min filtration. The SDBS retention of the 20%-silica/titania nanorods/nanotubes composite membrane is relatively high, which is mainly due to small pore size and much better adsorption capability of the 20%-silica/titania nanorods/nanotubes composite membrane.

3.3. Photocatalytic activity

The photocatalytic activity of 20%-silica/titania nanorods/nanotubes composite membranes was investigated by the degradation experiment using SDBS as a test pollutant. After

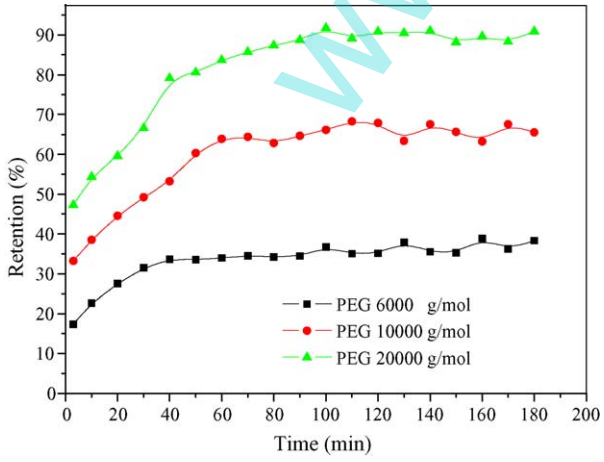

Fig. 6. PEG retention of the 20%-silica/titania composite membrane at a pressure difference of 0.05 MPa and a PEG concentration of 500 mg/L.

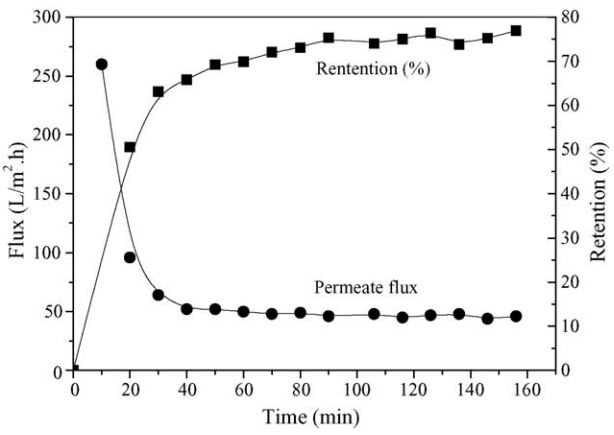

Fig. 7. SDBS permeate flux and retention of the 20%-silica/titania composite membrane at pH 3.5. A pressure difference of 0.05 MPa and a SDBS concentration 50 mg/L.

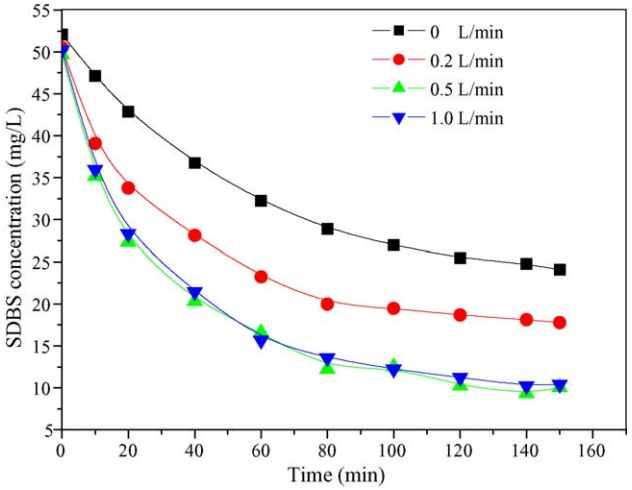

Fig. 8. SDBS concentration as function of UV irradiation time at different airflow. Initial pH 3.5; the initial concentration of SDBS 50 mg/L.

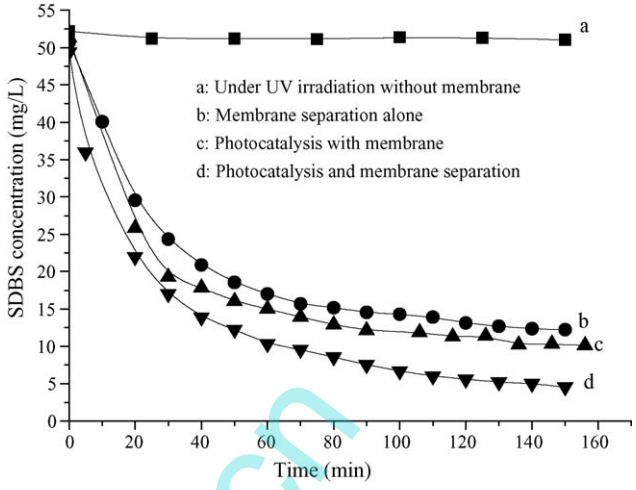

Fig. 9. (a–d) Concentration of SDBS solution versus time under different conditions. $V = 1000$ mL; $T = 298$ K; $C_{feed} = 50$ mg/L; initial pH 3.5; air flow = 0.5 L/min; $\Delta P = 0.05$ MPa.

30 min in darkness, the lamp was switched on and SDBS samples were periodically withdrawn for analysis.

The sensitivity of photocatalytic reaction to the availability to oxygen is well known. Haarstrick et al. [26] reported that oxygen is the key molecule for hydrogen peroxide (H_2O_2) formation and has a great effect on photocatalytic reaction. Oxygen is well known for scavenging the photogenerated electrons (Eq. (1)), impeding the hole–electron pair recombination process (Eq. (2)) and freeing up the photogenerated holes for further reactions. Thus, sufficient oxygen is important for successful and efficient photocatalysis. In our experiment, air was bubbled simply into the solution. It had two important functions: supplied oxygen and stirred solution. Air flow, during the process of photocatalytic reaction, has been studied (shown in Fig. 8). As shown, the efficiency of photocatalytic reaction increases as air flow increases. However, the photocatalytic efficiency is very close at air flow of 0.5 and 1.0 L/min. The reason may be that oxygen is sufficient for photocatalytic reaction at air flow of 0.5 L/min. Therefore, excessive air can not improve the photocatalytic efficiency.

$$O_2 + e^- \rightarrow O_2^{\bullet -} \quad (1)$$

$$e^- + h^+ \rightarrow \text{heat} \quad (2)$$

3.4. Coupling photocatalysis and membrane techniques experiments of 20%-silica/titania nanorods/nanotubes composite membrane

The removal of SDBS was tested using 20%-silica/titania nanorods/nanotubes composite membrane in the continuous system. For this system, the following experimental conditions were used, i.e. 1000 mL of aqueous solution containing the SDBS (50 mg/L) at 298 K and pressure difference of 0.05 MPa; air flow 0.5 L/min; initial pH 3.5; in the experiment, the lamp was switched on after 30 min of mixing and running in darkness (time needed for air saturation of the solution and the achievement of steady-state conditions for the adsorption phenomena). The concentrations of the SDBS in the retentate and permeate were periodically analysed by spectrophotometer.

The SDBS in water has a strong absorption peak at 224 nm (UV absorption of the aromatic group). No significant direct photolysis of SDBS occurred in the absence of 20%-silica/titania nanorods/nanotubes composite membrane (Fig. 9a). The removal of SDBS with membrane separation alone reached 74% after 100 min filtration (Fig. 9b) and this removal of the SDBS should include two aspects, adsorption (physical and chemical) and mechanical retention. The SDBS adsorption on the surface of composite membrane is 11% after 100 min. When 20%-silica/titania nanorods/nanotubes composite membrane was used as photocatalytic membrane, the SDBS can be decomposed under UV irradiation (Fig. 9c). The removal of SDBS achieved 78% after 100 min UV irradiation. It can be seen from Fig. 9d that the removal efficiency of SDBS was improved using photocatalysis coupled with membrane technology. The removal of SDBS achieved 89% after 100 min. The above results implied that the 20%-silica/titania nanorods/nanotubes composite membrane possessed much better photocatalytic activity and membrane separation capability. The multifunctions of photocatalysis and membrane separation can be realized using 20%-silica/titania nanorods/nanotubes composite membrane.

4. Conclusions

The above discussion demonstrated that embedding amorphous silica into titania matrix resulted in suppressing the titania phase transformation from anatase to rutile and inhibiting titania particles increase. The small size titania particles with anatase phase play an important role in formation of silica/titania nanotubes composite membrane with photocatalytic capability. Moreover, material properties of composite membrane (such as thermal stability) were improved and its photocatalytic activity was apparently enhanced by embedding amorphous silica into titania matrix. The experimental results

showed that combining the photocatalysis with membrane techniques removed organic pollutants from wastewater and the removal efficiency was improved markedly. At the same time, good photocatalytic capability of silica/titania nanorods/nanotubes composite membrane improved permeation flux of composite membrane and prevented composite membrane fouling.

In a summary, according to our research, the silica/titania nanorods/nanotubes composite membranes have the multi-functions of photocatalysis and separation simultaneously. Coupling photocatalysis and membrane techniques result a very powerful process with a great innovation in water purification. Such an innovation has important significance in exploring a new efficient method to solve water pollution problem. This approach could be interesting by an application point of view to use photocatalysis coupled with membrane technology for the decontamination of actual effluents produced in many industries.

Acknowledgments

The authors would like to thank National Basic Research Program of China (Project No. 2003CB415006) and National Nature Science Foundation of China (No. 20337020) for financial support.

References

[1] C.A.K. Gouvea, F. Wypych, S.G. Moraes, N. Duran, N. Nagata, P. Peralta-Zamora, Chemosphere 40 (4) (2000) 433–440.
[2] W.Z. Tang, H. An, Chemosphere 31 (9) (1995) 4157–4170.
[3] I. Voigt, G. Fischer, P. Puhlfürβ, M. Schleifenheimer, M. Stahn, Sep. Purif. Technol. 32 (2003) 87–91.
[4] A.L. Ahmad, M.R. Othman, H. Mukhtar, Int. J. Hydrogen Energy 29 (2004) 817–828.
[5] I. Voigt, M. Stahn, St. Wöhner, A. Junghans, J. Rost, W. Voigt, Sep. Purif. Technol. 25 (2001) 509–512.
[6] L. Xu, W.P. Li, S.Q. Lu, Z. Wang, Q.X. Zhu, Y. Ling, Desalination 149 (2002) 199–203.
[7] C. Combe, C. Guizard, P. Aimar, V. Sanchez, J. Membr. Sci. 129 (1997) 147–160.
[8] O.K. Varghese, D.W. Gong, M. Paulose, K.G. Ong, E.C. Dickey, C.A. Grimes, Adv. Mater. 15 (2003) 624–627.
[9] S. Livraghi, A. Votta, M.C. Paganini, E. Giamello, Chem. Commum. 4 (2005) 498–500.
[10] A. Hagfeldt, M. Gratzel, Acc. Chem. Res. 33 (2000) 269–277.
[11] A. Hagfeldt, M. Gratzel, Chem. Rev. 95 (1995) 49–68.
[12] Y.S. Chen, J.C. Crittenden, S. Hackney, L. Sutter, D.W. Hand, Environ. Sci. Technol. 39 (2005) 1201–1208.
[13] S. Ahuja, T.R.N. Kutty, J. Photochem. Photobiol. A: Chem. 97 (1996) 99–107.
[14] M. Anpo, H. Nakaya, S. Kodama, Y. Kubokawa, J. Phys. Chem. 90 (1986) 1633–1636.
[15] C. Anderson, A.J. Bard, J. Phys. Chem. 99 (1995) 9882–9885.
[16] T. Takata, K. Shinohara, A. Tanaka, M. Hara, J.N. Kondo, K. Domen, J. Photochem. Photobiol. A: Chem. 106 (1997) 45–49.
[17] W. Zhao, W.H. Ma, C.C. Chen, J.C. Zhao, Z.G. Shuai, J. Am. Chem. Soc. 126 (2004) 4782–4783.
[18] X.D. Wang, P.X. Gao, J. Li, C.J. Summers, Z.L. Wang, Adv. Mater. 14 (2002) 1732–1735.
[19] X. Fu, L.A. Clark, Q. Yang, M.A. Anderson, Environ. Sci. Technol. 30 (1996) 647–653.
[20] H.Z. Zhang, X.H. Luo, J. Xu, B. Xiang, D.P. Yu, J. Phys. Chem. B 108 (2004) 14866–14869.
[21] H. Hidaka, J. Zhao, E. Pelizzetti, N. Serpone, J. Phys. Chem. 96 (1992) 2226–2230.
[22] J. Zhao, H. Oota, H. Hidaka, E. Pelizzetti, N. Serpone, J. Photochem. Photobiol. A: Chem. 69 (1992) 251–256.
[23] K.Y. Jung, S.B. Park, Appl. Catal. B: Environ. 25 (2000) 249–256.
[24] J.J. Sene, W.A. Zeltner, M.A. Anderson, J. Phys. Chem. B 107 (2003) 1597–1603.
[25] S. Singh, K.C. Khulbe, T. Matsuura, P. Ramamurthy, J. Membr. Sci. 142 (1998) 111–127.
[26] A. Haarstrick, O.M. Kut, E. Heinzle, Environ. Sci. Technol. 30 (3) (1996) 817–824.